Actuability of Underactuated Manipulators

Christopher Lee Yangsheng Xu

CMU-RI-TR-94-13

The Robotics Institute
Carnegie Mellon University
Pittsburgh, PA 15213

June, 1994

©1994 Carnegie Mellon University

The views and conclusions contained in this document are those of the authors and should not be interpreted as representing the official policies or endorsements, either expressed or implied, of Carnegie Mellon University.

Abstract

In this paper we study underactuated manipulator systems, which are composed of both active and passive joints. The study of underactuated systems is interesting for a variety of applications including space robots, hyperredundant robots, and mobile robots. When one or more joints in a normal manipulator system fail, control techniques for the resulting underactuated system can make use of dynamic coupling within the system for position control. In this paper, we define a performance measure for the motion of these underactuated manipulator systems. We call this performance measure *actuability*. Actuability is a measure of the ability of the actuators in a robot manipulator to cause acceleration of the end-effector. Based on this concept, we develop sensitivity analysis of the system's performance with respect to geometric and dynamics parameters of the robot. This investigation is significant for the design and control of an underactuated robot system.

Contents

1 Introduction **1**

2 Actuability **2**

2.1 Dynamics Based on the Jacobian 2

2.2 Actuability Matrix 4

2.3 Actuability Ellipsoid 5

2.4 Scalar Measures of Actuability 6

3 Simulation Study **8**

3.1 Actuability Index 8

3.2 Actuability Ellipsoid 9

4 Sensitivity Analysis **13**

4.1 Sensitivity to Link Masses 14

4.2 Sensitivity to Loading 16

4.3 Sensitivity to Kinematic Parameters 17

5 Conclusion **20**

List of Figures

1 w_{u1} and w_{u2} of upper-actuated manipulators 8
2 w_{u1} and w_{u2} of lower-actuated manipulators 9
3 Actuability ellipsoids of manipulators with 1 actuator 10
4 Child on swing 12
5 Actuability ellipsoids of manipulators with 2 actuators 12
6 Actuability ellipsoids of manipulators with 3 actuators 12
7 Actuability sensitivity to link masses: 2 lower-actuators 14
8 Actuability sensitivity to link masses: 3 lower-actuators 14
9 Actuability sensitivity to link masses: 2 upper-actuators 15
10 Actuability sensitivity to link masses: 3 upper-actuators 15
11 Actuability sensitivity to load masses: 2 lower-actuators 16
12 Actuability sensitivity to load masses: 3 lower-actuators 17
13 Actuability sensitivity to load mass: 2 actuators 17
14 Sensitivity to l_1 for lower-actuated manipulator with 3 actuators 18
15 Sensitivity to l_1 for upper-actuated manipulator with 3 actuators 18

1 Introduction

Researchers have recently begun studying robotic manipulators with more joints than actuators. These devices, which are commonly referred to as 'underactuated manipulators' [1] [2], are interesting because they allow us to investigate several important kinds of manipulation. For space robotics scenarios where failed actuators cannot easily be repaired, we are interested in knowing how well we can control the arm with the remaining actuators. It is also conceivable that a space manipulator should be be designed with less actuators than joints if it were determined that such a configuration retained most of the usefulness of a fully actuated manipulator, while weighing less and using less power. In addition to potentially helping with fault tolerance, weight-reduction, and energy efficiency in space robots, the study of underactuated manipulation can help us to better understand and possibly recreate natural motion. When a person walks, a monkey swings through trees, or a child rides a swing, there are often 'joints' which are not actuated during part or all of the motion [3] [1]. The late movie star Bruce Lee, through his precise control of the placement of the tips of a pair of 3-link numbchucks, as well as his ability to control impact force at these tips, presents an example of the potential effectiveness of such hybrid passive/active mechanisms. For hyper-redundant robot systems, such as snake-robots, it is certainly desirable for some of the joints to be passive if it can be determined that the robot is still fully controllable.

One of the most basic questions in the study of any manipulator is simply "How effective are the joint-actuators in causing motion at the end-effector?" For a fully-actuated manipulator, such questions are generally answered by investigating the dynamic manipulability ellipsoid of the manipulator [4]. Dynamic manipulability is a useful measure of both the relative magnitude of the manipulator's ability to cause acceleration in a certain configuration, and also of the degree of dependence that the magnitude of the achievable acceleration has on the direction of that acceleration. In the case of the underactuated manipulator, however, the concept of dynamic manipulability needs to be developed further to be a useful measure in answering the same fundamental question.

In this paper, we develop a measure that is actually an indication of the arbitrariness of the actuators' ability to cause acceleration at the end-effector in an underactuated robot system. We call the measure the *actuability* of a manipulator in a given configuration. Based on this concept, the robot's geometric parameters and dynamic properties can be optimally determined in the sense of maximizing actuability. The robot's control-input profile can be optimally planned to avoid potential singularities. Moreover, the maximum payload capacity and the effect of payload on system performance can be easily understood using actuability.

2 Actuability

There are two common forms of manipulability measures for manipulators: kinematic manipulability, and dynamic manipulability [4]. Kinematic manipulability is a characterization of a manipulator which is based on the singular-value decomposition of the manipulator's Jacobian matrix, defined in (3). Dynamic manipulability is similar to kinematic manipulability, but takes the inertial matrix of the manipulator into account as well.

The derivation of the actuability measure is initially similar to that of dynamic manipulability. This is because a purely kinematics-based measure is of far less interest than a dynamics-based one for underactuated manipulators. An underactuated manipulator cannot be directly controlled in the position or the velocity domains, because the unactuated joints must be controlled through the dynamic coupling effects that operate between links of the manipulator. Coupling forces between the actuated and unactuated joints of an underactuated manipulator are of two main types: those which can be produced by actuators, and those which cannot. For a characterization of actuability, then, we begin with the basic dynamic equation of a manipulator.

2.1 Dynamics Based on the Jacobian

Through a Newton-Euler or a Lagrangian derivation, we can determine the basic equation for the dynamics of a serial manipulator to be

$$\tau = M(q)\ddot{q} + h(q, \dot{q}) + G(q), \tag{1}$$

where $M(q)$ is the inertial matrix of the manipulator, $h(q, \dot{q})$ represents the Coriolis and centrifugal forces, and $G(q)$ is the gravitational force acting on the manipulator.

If the manipulator is partitioned into an actuated part with n_a actuated joints and an unactuated part with n_p unactuated joints, we can partition (1) as follows:

$$\begin{bmatrix} \tau_a \\ \tau_p = 0 \end{bmatrix} = \begin{bmatrix} M_{aa} & M_{ap} \\ M_{pa} & M_{pp} \end{bmatrix} \begin{bmatrix} \ddot{q}_a \\ \ddot{q}_p \end{bmatrix} + \begin{bmatrix} h_a \\ h_a \end{bmatrix} + \begin{bmatrix} G_a \\ G_p \end{bmatrix} \tag{2}$$

where the inertial matrix of the actuated part M_{aa} is an $n_a \times n_a$ submatrix of M, the inertial matrix of the unactuated part M_{pp} is an $n_p \times n_p$ submatrix of M, and the coupling matrices M_{ap} and M_{pa} are $n_a \times n_p$ and $n_p \times n_a$ submatrices of M, respectively. Note that this expression describes any robot configuration with mixed passive and active joints in a series mechanism. Because we partition the matrices so that the equations representing the active joints are in the top rows while the equations representing the passive joints are in the bottom rows, the matrix M is not a conventional inertial matrix of a serial-chain manipulator. Therefore, this expression will be valid for general

underactuated systems. For the special case of 'lower-actuated' configurations, where all passive joints are located near the base of the mechanism, the matrix M is a conventional inertial matrix. Also note that M_{aa} and M_{pp} are always square matrices, but M_{pa} and M_{ap} are normally not square.

In equations (1) and (2), the values of the nonlinear velocity-related matrix $h(q, \dot{q})$ and the gravitational force matrix $G(q)$ are determined by geometric configuration and joint velocities $(q, \dot{q})$ only. In our analysis, we will be more concerned with the effects of the joint torques τ on the acceleration of the joints $\ddot{q}$ than the effects of gravitational and nonlinear forces. While we can directly control the actuator torques in the active joints, we cannot directly affect the gravitational, Coriolis, and centrifugal forces in the system. Thus, we subtract the gravitational and nonlinear forces from τ, resulting in a linear relationship in terms of 'virtual torque'.

The relationship between end-effector velocity and actuator velocity is given by the Jacobian $J = [J_a \ J_p]$ such that

$$J_{ij} = \frac{\partial x_i}{\partial q_j}. \tag{3}$$

Note that J_a, which describes the relationship between end-effector velocity and the velocity of the active joints, is a $(d_w \times n_a)$ matrix and J_p, the relationship between the end-effector velocity and the joint velocity of the unactuated joints, is a $(d_w \times n_p)$ matrix, where d_w is the number degrees of freedom of the workspace or the number of manipulation variables. In this case, as in the case of M, J is not a conventional Jacobian matrix due to its reorganization for the purpose of partitioning it into active and passive parts.

The Jacobian allows us to write

$$\dot{X} = J(q)\dot{q} \tag{4}$$

$$\dot{v} = \ddot{X} = J(q)\ddot{q} + a_r(q, \dot{q}) \tag{5}$$

where $a_r = \dot{J}(q)q$ can be interpreted as the virtual acceleration caused by the nonlinear relationship between the two coordinate systems for q and r. Following the derivation by Yoshikawa [4],

$$\begin{aligned} a_r &= JJ^+a_r + (I - JJ^+)a_r \\ &= JM^{-1}MJ^+a_r + (I - JJ^+)a_r, \end{aligned} \tag{6}$$

we obtain from (1) and (5) the relationship:

$$\dot{v} - (I - JJ^+)a_r = JM^{-1}[\tau - h(q, \dot{q}) - g(q) + MJ^+a_r]. \tag{7}$$

where the torques due to the Coriolis force, centrifugal force, and gravitational force, and (MJ^+a_r), which are *joint-generable* torques due to the nonlinear-relationship between the coordinate systems of q and v, are subtracted from the actuator torque τ. In addition, all the accelerations which are

not producible by joint motion, $(I - J^+J)a_r$, are subtracted from the Cartesian acceleration term $\dot{v}$. Note that if the actuator is not in a kinematically singular configuration, then $I - J^+J = 0$.

We define the virtual torque as

$$\tilde{\tau} = \tau - h(q, \dot{q}) - g(q) + MJ^+a_r. \tag{8}$$

This is the physical joint-torque without Coriolis, gravitational, or centrifugal forces, and with the nonlinear torques due to the mapping from Cartesian space to joints space added-in. Next, we define the virtual acceleration

$$\tilde{\dot{v}} = \dot{v} - (I - JJ^+)a_r, \tag{9}$$

which is physical acceleration of the end-effector minus any acceleration in directions which cannot be affected by joint torques (due to kinematic singularities). We can now rewrite (7) as

$$\tilde{\dot{v}} = (JM^{-1})\tilde{\tau}. \tag{10}$$

For fully-actuated manipulators, the dynamic manipulability measure is based-on this equation. In these systems, we generally analyze the manipulator performance in terms of the 'dynamic manipulability ellipsoid', which is the possible range of acceleration such that

$$\tilde{\dot{v}}(J^+)^T M^T (MJ^+)\tilde{\dot{v}} \leq 1. \tag{11}$$

2.2 Actuability Matrix

The dynamic manipulability measure shows how well each joint can generate motion (in terms of acceleration) at the end-effector. In the case of underactuated manipulators, however, not all of the joints are actively controllable. Therefore we need a measure to evaluate how well active joints can generate end-effector motion, or how strong the dynamic coupling is from active joint motion to end-effector motion. To this end, we derive a new concept, *actuability*, for characterization of underactuated manipulator systems.

We first decompose (10) as

$$\tilde{\dot{v}} = [J_a\ J_p] \begin{bmatrix} \phi_{aa} & \phi_{ap} \\ \phi_{pa} & \phi_{pp} \end{bmatrix} \begin{bmatrix} \tilde{\tau}_a \\ \tilde{\tau}_p \end{bmatrix} \tag{12}$$

$$\phi = M^{-1} = \begin{bmatrix} \phi_{aa} & \phi_{ap} \\ \phi_{pa} & \phi_{pp} \end{bmatrix}. \tag{13}$$

If $n_a \geq n_p$, we can calculate ϕ using the formula,

$$\phi = \begin{bmatrix} \tilde{M}_{aa}^{-1} & -\tilde{M}_{aa}^{-1} M_{ap} M_{pp}^{-1} \\ -M_{pp}^{-1} M_{pa} \tilde{M}_{aa}^{-1} & M_{pp}^{-1} + M_{pp}^{-1} M_{pa} \tilde{M}_{aa}^{-1} M_{ap} M_{pp}^{-1} \end{bmatrix} \tag{14}$$

$$\tilde{M}_{aa} = M_{aa} - M_{ap} M_{pp}^{-1} M_{pa}, \tag{15}$$

or if $n_p > n_a$,

$$\phi = \begin{bmatrix} M_{aa}^{-1} + M_{aa}^{-1} M_{ap} \tilde{M}_{pp}^{-1} M_{pa} M_{aa}^{-1} & -M_{aa}^{-1} M_{pa} \tilde{M}_{pp}^{-1} \\ -M_{aa}^{-1} M_{ap} \tilde{M}_{pp}^{-1} & \tilde{M}_{pp}^{-1} \end{bmatrix} \quad (16)$$

$$\tilde{M}_{pp} = M_{pp} - M_{pa} M_{aa}^{-1} M_{ap}. \quad (17)$$

We can then write

$$\tilde{\dot{v}} = \begin{bmatrix} J_a \phi_{aa} + J_p \phi_{pa} & J_a \phi_{ap} + J_p \phi_{pp} \end{bmatrix} \begin{bmatrix} \tilde{\tau}_a \\ \tilde{\tau}_p \end{bmatrix} \quad (18)$$

$$= (J_a \phi_{aa} + J_p \phi_{pa}) \tilde{\tau}_a + (J_a \phi_{ap} + J_p \phi_{pp}) \tilde{\tau}_p. \quad (19)$$

$$= A_u \tilde{\tau}_a + B_u \tilde{\tau}_p \quad (20)$$

In (19), the term $(J_a \phi_{aa} + J_p \phi_{pa}) \tilde{\tau}_a = A_u \tilde{\tau}_a$ represents the part of virtual acceleration which the actuators can produce, and the other term $(J_a \phi_{ap} + J_p \phi_{pp}) \tilde{\tau}_p = B_u \tilde{\tau}_p$ represents the part of the virtual acceleration which is due entirely to apparent forces in the unactuated joints.

We are only interested in $A_u \tilde{\tau}_a$, because it is this term which describes the ability of actuator torques to induce acceleration in the manipulator. We want to determine the arbitrariness of the acceleration which can be achieved through actuation. Just like gravitational, Coriolis, and centrifugal forces which were discounted in "virtualizing" the torque, the forces $B_u \tilde{\tau}_p$, which are functions only of joint position and velocity $(q, \dot{q})$, are non-controllable and thus not interesting for an actuability measure. The matrix $A_u = (J_a \phi_{aa} + J_p \phi_{pa})$, on the other hand, directly relates virtual torque and virtual acceleration. We call A_u the *actuability matrix* in this paper. We can investigate the actuability matrix in the same way that the matrix JM^{-1} is used for analyzing the dynamic manipulability of fully actuated manipulators. This actuability matrix can also be written in a more general form as,

$$A_u = J \ (M^{-1} \text{diag}[k(1), \ k(2), \ \ldots \ , k(n_a + n_p)]) \quad (21)$$

where $k(i)$ is 1 if the ith joint is actuated and 0 if the ith joint is unactuated.

2.3 Actuability Ellipsoid

We want to develop a measure of how well acceleration in the end-effector can be generated given the allowable input torque on the active joints. For this purpose, we use a unit torque $||\tilde{\tau}_a|| \leq 1$. The set of end-effector accelerations this set of torques can produce is an ellipsoid in d_w-dimensional space given by

$$\tilde{\dot{v}}^T (A_u^+)^T A_u^+ \tilde{\dot{v}} \leq 1, \ \ \tilde{\dot{v}} \in \text{R}(J). \quad (22)$$

This ellipsoid is called the *actuability ellipsoid*.

Let the singular-value decomposition of the actuability matrix, A_u, be

$$A_u = U_u \Sigma_u V_u^T \tag{23}$$

where $\Sigma_u = [\text{diag}(\sigma_{u1}, \ldots, \sigma_{ud_w}) \,|\, 0]$, $\sigma_{u1} > \sigma_{u2} > \ \ldots \ > \sigma_{ud_w}$, and the orthonormal matrix $U_u = [u_{u1}, \ldots, u_{ud_w}]$. The principal axes of the actuability ellipsoid are

$$\sigma_{u1} u_{u1}, \ \sigma_{u2} u_{u2}, \ \ldots, \ \sigma_{ud_w} u_{ud_w}.$$

The actuability ellipsoid can be interpreted in the same way as the dynamic manipulability ellipsoid. If the ellipsoid for a given configuration is of a generally large size, that means that the actuators should be able to produce a large acceleration of the end-effector. The greatest acceleration of the end-effector can be produced in the direction of the major axis of the actuability ellipsoid, and the least acceleration can be produced along the minor axis. If the size of one of the axes of the actuability ellipsoid goes to zero, then the actuability matrix is singular, and the manipulator cannot cause acceleration of the end-effector in an arbitrary direction.

2.4 Scalar Measures of Actuability

To use the actuability ellipsoid for real-time control, or to perform off-line optimization of manipulator kinematic-redundancy for following end-effector trajectories, we would like to have characterizations of actuability in a scalar form. One such useful measure is the volume of the ellipsoid. If the value of this scalar measure ever falls to zero, then we are at a singular configuration with respect to actuability. The volume of the actuability ellipsoid can be shown to be proportional to the quantity $\sqrt{\det[A_u^T A_u]}$, or $\sqrt{\det[A_u A_u^T]}$ if A has more rows than columns. Matrix A has more rows than columns whenever $n_a < d_w$.[1] Figure 3 shows two such manipulator configurations. In these cases, the manipulability measure w_{u1} is proportional to the *length* of the line segment that is a one-dimensional version (because of the single actuator) of the manipulability ellipsoid. The length of this line segment should never be directly compared to a higher-dimensional measure such as the area of a 2-D actuability ellipse.

Another useful measure is a quantity related to the shape of the actuability ellipsoid. If the ratio of the lengths of the shortest and greatest axes of the manipulability ellipsoid is low, then we know

[1] Note that the conditions for the use of the second expression, $\sqrt{\det[A_u A_u^T]}$, already imply that the manipulator is always 'singular' with respect to workspace dimensionality, and thus this measure is proportional to a lower-dimensional version of the manipulability ellipsoid. If this quantity goes to zero, we have an even stronger kind of singularity.

that the ability of the actuators to cause acceleration of the end-effector is highly dependent upon the direction of the desired acceleration. We also know that the error-sensitivity of the end-effector acceleration is highly dependent upon this ratio. In fact, it can be shown that

$$\frac{1}{\sigma_{u1}} \leq \frac{||\Delta\tilde{\dot{v}}||}{||\Delta\tilde{\tau}_a||} \leq \frac{1}{\sigma_{ud_w}}, \tag{24}$$

where $\Delta\tilde{\tau}_a$ is the error in actuator torque and $\Delta\tilde{\dot{v}}$ is the resulting error in end-effector acceleration.

Therefore, we have the following scalar actuability measures:

$$w_{u1} = \begin{cases} \sqrt{\det[A_u^T A_u]} & \text{if } n_a > d_w \\ |\det[A_u]| & \text{if } n_a = d_w \\ \sqrt{\det[A_u A_u^T]} & \text{if } n_a < d_w \end{cases} \tag{25}$$

$$w_{u2} = \sigma_{ud_w}/\sigma_{u1}. \tag{26}$$

For the purpose of maximum actuability, we would like w_{u1} to be as great as possible, and for the purpose of limiting error sensitivity, we would like w_{u2} to be as close to one as possible. One approach for controlling a redundant underactuated manipulator might be to check these quantities periodically, and once w_{u1} or w_{u2} drops below a certain threshold, to use the offending quantity as part of a redundant control algorithm which attempts to return the quantity to a safe value while maintaining the desired trajectory as closely as possible. Note that as $w_{u2} \rightarrow 0$, we know that $w_{u1} \rightarrow 0$ (see figures 1 and 2), so in extreme cases we need only optimize for one actuability measure at a time.

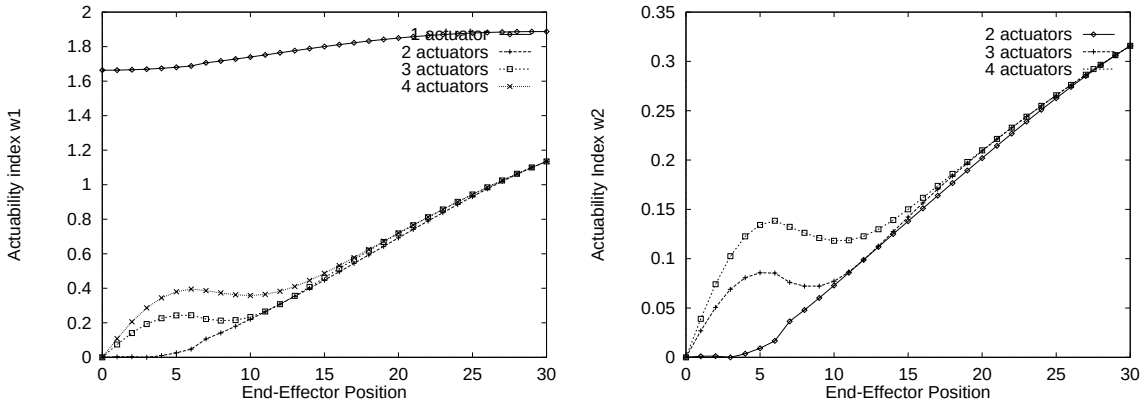


Figure 1: Actuability index comparison: w_{u1} (left) and w_{u2} (right) of upper-actuated manipulators

3 Simulation Study

3.1 Actuability Index

Here are some results from simulations of a simple four-link planar manipulator with the following geometric and dynamic specifications:

link	l	l_c	I	m
1	1.0	0.5	0.3	1.0
2	1.0	0.5	0.3	1.0
3	1.0	0.5	0.3	1.0
4	1.0	0.5	0.3	1.0

For observing the evolution of the actuability ellipsoid over a trajectory, we investigate a trajectory generated by constraining the joints to have the same angle, $q_1 = q_2 = q_3 = q_4$ where q_i is the angle of the ith joint from the base, and varying this angle from 0.0 to 1.55 radians.

Figures 1 and 2 show the values of the actuability ellipsoid along the demonstration trajectory for manipulators with different numbers of actuators, and for manipulators that are upper-actuated, where actuators are in the joints nearest the end-effector, and lower-actuated, where actuators are in the joints nearest the base. Later figures diagram in more detail the evolution of the ellipsoids. *Note that the 1-actuator plots of the first plots in Figures 1 and 2 show a fundamentally different quantity than the 2-, 3-, and 4-actuator plots.* The 1-actuator plots show w_{u1} relating to the *length* of the 1-D actuability ellipsoid, while the other plots show w_{u1} relating to the *area* of the 2-D ellipsoid. This is why in the first plot of Figure 1, the 1-actuator plot does not register the kinematic singularity that the other plots show for 'end-effector position 0', the straight-manipulator configuration.

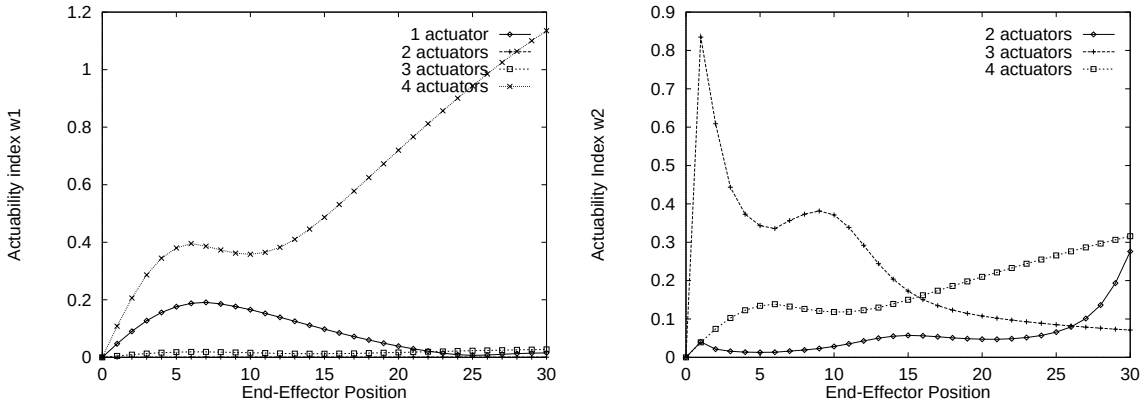


Figure 2: Actuability index comparison: w_{u1} (left) and w_{u2} (right) of lower-actuated manipulators

The actuability-index figures show that, in general, tip acceleration is more easily generated by upper-actuated manipulators (w_{u1} up to 1.0) than by lower-actuated manipulators (w_{u1} up to 0.2). This is not surprising when it is considered that the effect of all torques in the actuators are equally weighted in the current actuability indices, and that actuators near the base must cause acceleration of the entire arm to achieve acceleration at the end-effector, while actuators near the effector must only accelerate a small portion of the manipulator to achieve acceleration at the tip. It should prove true, however, that this ability of upper-actuated manipulators to cause acceleration at the tip is most useful locally, but less useful for coarse motion from one tip-location to another across the workspace. This would be a good subject for a more formal investigation.

We can see in the first plot of Figure 2 that index w_{u1} for the lower-actuated manipulators was zero at the singularity, rose to a maximum around end-effector position 6, and then fell again. The low value of the manipulability index in the lower-actuated manipulators when the arm is curled is in contrast to the behavior of the index for the upper-actuated manipulator. This suggests that the actuators at the base of the manipulator are applying effective torques on the arm *around* the end-effector rather then applying force *at* the end-effector.

Figures 3, 5, and 6 show the actuability ellipsoid at the end-effector of lower- and upper-actuated manipulators with 1, 2, and 3 actuated joints.

3.2 Actuability Ellipsoid

The first plot of Figure 3 shows the actuability of a manipulator with a single actuator in the joint nearest the end-effector. The plot makes intuitive sense in that the ellipsoid is always 1-dimensional, of almost constant length, and is almost perpendicular to the long axis of the last link. A torque in the actuator will produce a motion in the last link, and a less-significant motion

(due to greater rotational inertia) in the rest of the arm as a whole. Any deviation in direction of end-effector acceleration from the perpendicular to the long axis of the last link will be due to the smaller acceleration of the rest of the arm.

Contrast this to the second plot of Figure 3, showing a manipulator with a single actuator in the joint at the base. We see that the alignment of the 1-D actuability ellipsoid is generally close to the major axis of the last link rather than perpendicular to it. We can see from Figure 2 that the actuability measure w_{u1} varies between 0.0 and 0.2 for the lower-actuated manipulator as opposed to the upper-actuated manipulator where w_{u1} varies between 1.6 and 1.8 along the same trajectory (see Figure 1). The ability of an actuator at the base to generate acceleration at the tip of the robot is hindered by the large amount of manipulator mass that it has to move to cause motion in the end-effector. In addition, actuator torques cannot be directly transmitted to the end-effector because of the unactuated revolute joints between the end-effector and the actuator. Actuator force can be most effectively transmitted to the end-effector along the major axes of the links, because the passive joints do not transmit torques. Thus the actuability ellipse is generally aligned with the major axis of the last link. When the arm is curled at each joint, the link axes are not aligned, and it is difficult to transmit force along the links to the tip. Thus, at the more curled arm-configurations, the index w_{u1} approaches zero.

The upper-actuated manipulator is much like a child on a swing (see Figure 4), if we consider the connection between the chain and the supporting bar as one unactuated joint (joint 1), and the child's knee as an actuated joint (joint 2). We can consider the child's feet as the 'end-effector'. The child may easily accelerate her feet in Cartesian space by generating torques at the knees. In addition, through the coupling between the knee-joint (joint 2) and joint 1, she may swing without begin pushed by anyone. The actuable acceleration of the feet is at any given time almost

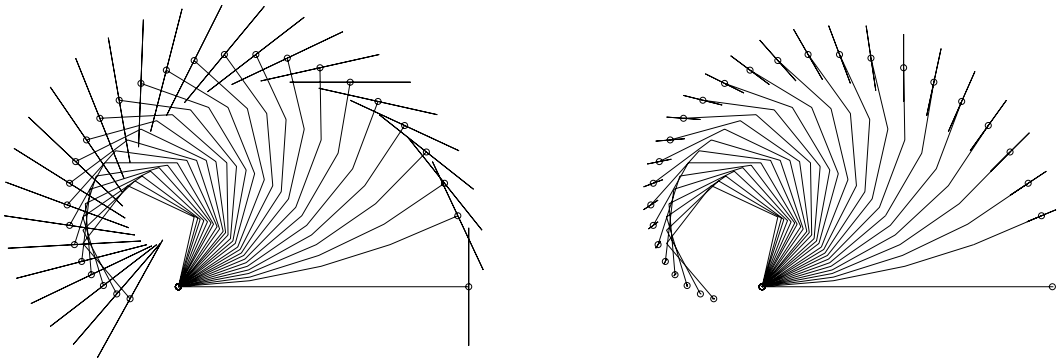


Figure 3: Actuability ellipsoids of manipulators with 1 actuator: left picture is upper-actuated, right is lower-actuated

perpendicular to the shins (link 2) and is fairly uniform at any given time. This matches our observations of Figure 3, and our conclusion that upper-actuation seems fairly effective in terms of actuability.

If the connection between the supporting bar and the swing is itself a rigid bar (instead of a chain), we can imagine trying to accelerate the child's feet by applying a torque at joint 1. Obviously, a torque at the child's knee is much more effective in accelerating her feet than the same torque at joint 1, due to the long lever-arm and the fact that we need to accelerate the child's entire body to accelerate her feet using joint 1. This is the basic reason that actuability is much smaller for lower-actuated manipulators. Note, however, that the scale of the motion that can be caused by joint 1 is much greater than the scale of the motion that can be caused by joint 2.

Figures 5 and 6 show the actuability ellipsoids for two- and three-actuator manipulators. Similar observations may be made about these manipulators and the single-actuator manipulators. Note that actuability of the upper-actuated manipulators is generally much greater than that of the lower-actuated manipulators. Moreover, the plots show that the major axis of the actuability ellipsoid of the lower-actuated manipulators is generally parallel to the major axis of the last link, while the major axis of the upper-actuated manipulator's actuability ellipsoid is generally perpendicular to the last link.

Adding another joint actuator to a lower-actuated manipulator generally improves actuability in all configurations. Adding another joint actuator to an upper-actuated manipulator generally improves actuability in the straighter configurations.

In design of an underactuated manipulator, as in most manipulators, it is probably a good idea to have stronger actuators in the joints nearer the base. For this reason, it might be a good idea to weigh the joint torques in the actuability index such that the torques of lower-actuators can be greater than torques at the upper actuators.

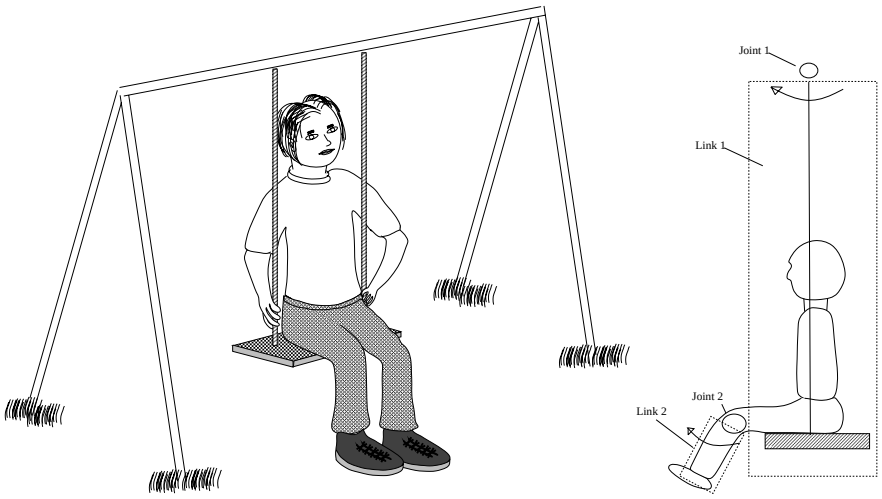


Figure 4: Child on a swing is much like a upper-actuated manipulator

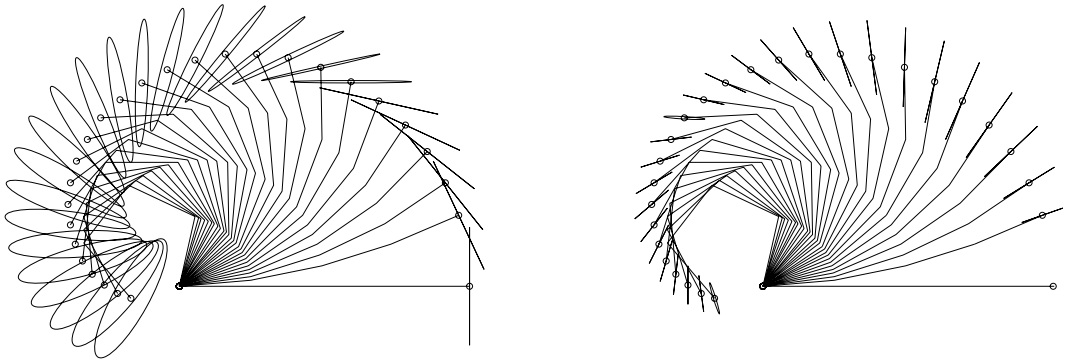


Figure 5: Actuability ellipsoids of manipulators with 2 actuators: left picture is is upper-actuated, right is lower-actuated

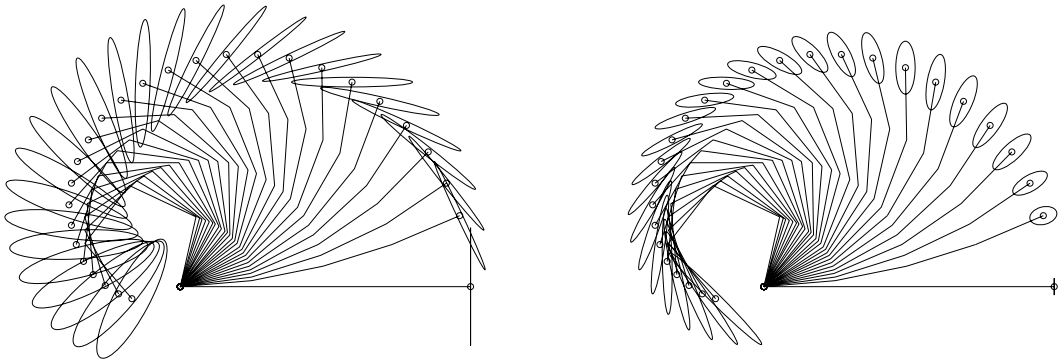


Figure 6: Actuability ellipsoids of manipulators with 3 actuators: left picture is is upper-actuated, right is lower-actuated

4 Sensitivity Analysis

Underactuated manipulators are generally difficult to control through model-based schemes, because the results are highly sensitive to modelling error. The difficulty lies in the fact that these schemes rely on manipulator models for both the dynamic feedforward term and the kinematic mapping from Cartesian space to joint space. The kinematic mapping here is related to dynamics, and any error in the dynamic parameters will cause error in joint control commands. For this reason, it is important to be able to determine the sensitivity of the behavior of a given manipulator with respect to functions such as modelling error or end-effector loading. It is still interesting to know this in cases where more robust control techniques are used, such as those in [2] and [1]. When, for example, the manipulator picks-up an object with a slightly different mass than expected, if the dynamics of the arm therefore vary significantly from what we are expecting, the arm will be very difficult to control until it drops the load.

Actuability represents a manipulator's ability to produce end-effector acceleration. Because this is a measure of dexterity in a dynamic sense, the sensitivity of a manipulator's actuability with respect to a given function of its parameters is a measure of the degree to which the local performance of the manipulator depends on that particular function. In designing an underactuated manipulator for configuration and geometric parameters, we may want to investigate the sensitivity of actuability with respect to the geometric parameters of the manipulator, and to the location of actuators in the mechanism. In motion planning for the robot, we may want to see the sensitivity of actuability to the manipulator's trajectory and use the sensitivity measure as a performance index for maximizing actuability. In controlling the robot, we may want to analyze the sensitivity of the robot motion with respect to the payload at the tip.

We define the sensitivity of a manipulator's actuability at a given configuration with the expressions

$$s_1 = \left. \frac{\partial w_{u1}}{\partial f} \right|_{f_o} \tag{27}$$

and

$$s_2 = \left. \frac{\partial w_{u1}/w_{u1}}{\partial f/f} \right|_{f_o} \tag{28}$$

where f is a function with respect to which we would like to measure sensitivity of actuability index w_{u1}. For simplicity, we only discuss the sensitivity of w_{u1}, although we can study sensitivity of w_{u2} in exactly the same way. Equation (27) is a measure of absolute sensitivity, while (28) is a relative measure. One measure may be better than the other for a given purpose, and other similar measures could be equally useful.

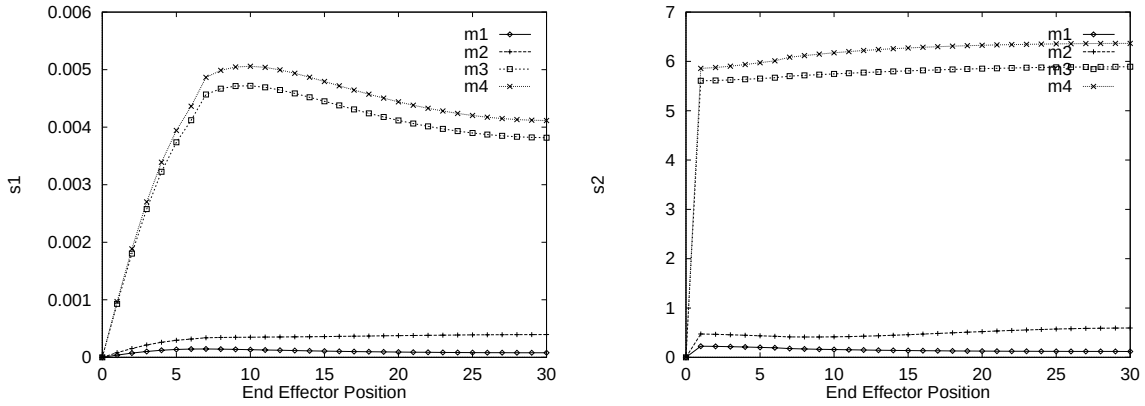


Figure 7: Sensitivities s_1 and s_2 to link masses for lower-actuated manipulator with 2 actuators

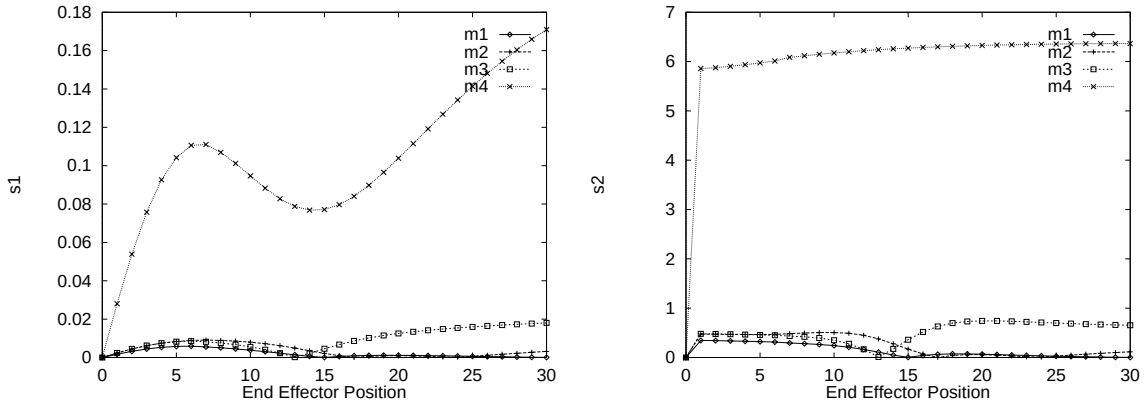


Figure 8: Sensitivities s_1 and s_2 to link masses for lower-actuated manipulator with 3 actuators

4.1 Sensitivity to Link Masses

Figures 7 through 10 are examples of sensitivity analysis with respect to errors in the manipulator model. Such analysis can be performed with respect to a number of relevant model parameters, such as the location of the center of gravity for a given link, the length of a link, or the inertia of a link. In this case, we choose to analyze the effect of modeling error in the link-mass parameters. The figures show the indices of equations (27) and (28) where the functions f are the values of the masses of each link.

In the plots of Figure 7, we see that for the lower-actuated manipulator with two actuators, the sensitivity is much greater for the masses of the unactuated links than for the actuated links. The same is true for the manipulator with three actuators, as is shown in Figure 8. Note that the sensitivity of the actuability at the singularity point (end-effector position zero) is always zero, because the actuability is zero at this point.

The sensitivity plots of the upper-actuated manipulators (Figures 9 and 10) are more compli-

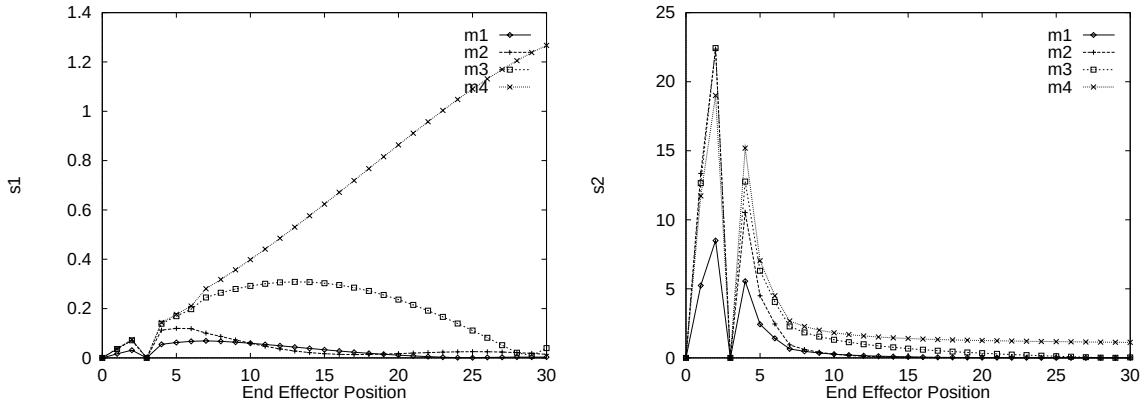


Figure 9: Sensitivities s_1 and s_2 to link masses for upper-actuated manipulator with 2 actuators

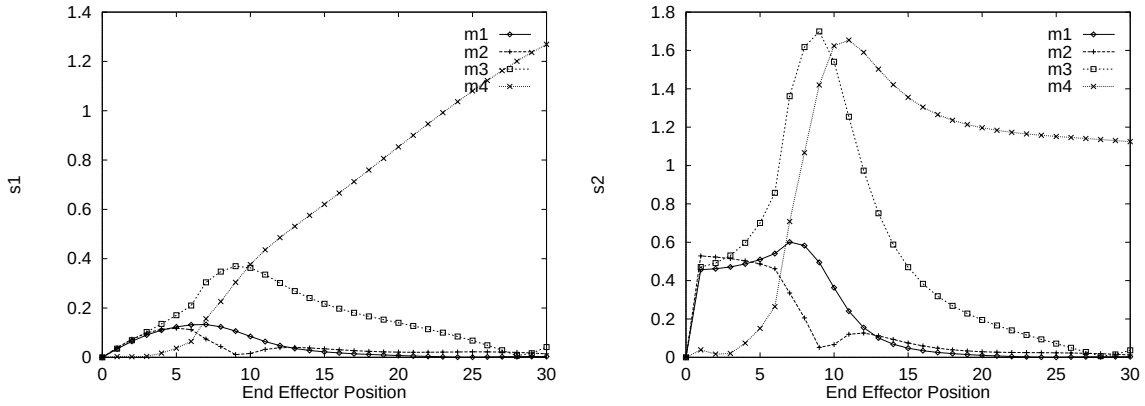


Figure 10: Sensitivities s_1 and s_2 to link masses for upper-actuated manipulator with 3 actuators

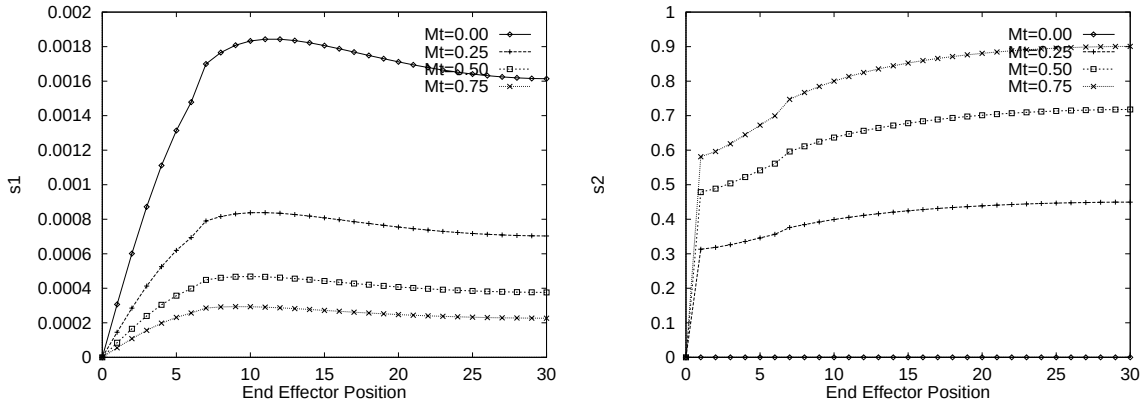


Figure 11: Sensitivities s_1 and s_2 to load mass for lower-actuated manipulator with 2 actuators

cated. Figure 9 shows wild fluctuations in *relative* sensitivity near the singularity point, but this is due to the fact that the absolute value of actuability in this region is very low (see Figure 1). As the arm becomes more curled, the relative sensitivity of the actuability decreases greatly. Figure 10 shows that the absolute sensitivity of the actuability of the upper-actuated manipulator with three actuators to link masses is almost the same as for the manipulator with two actuators, but the relative sensitivity is much lower due to the fact that the value of actuability index w_{u1} is generally much greater (see Figure 1). In both cases, the sensitivity of the actuability index to mass m_4 is much greater than the sensitivity to the other masses. This is due to the fact that the major axis of the actuability ellipsoid of these manipulators is generally perpendicular to the major axis of the last link (Figures 5 and 6), indicating that the greatest source of end-effector acceleration for these manipulators is the actuator at the last joint accelerating the last link. The actuability of the end-effector is thus closely related to the ability of the actuator in the last joint to cause acceleration in the last link, and is thus sensitive to the link's mass and the distance between the last joint and the last link's center of gravity.

4.2 Sensitivity to Loading

If the manipulator is used to pick-up and transport loads, it is useful to see how the amount of load at the end-effector affects the sensitivity of the manipulator's actuability to errors in the load-estimate. Figures 11 through 13 show these effects for upper- and lower-actuated manipulators with 2 actuators.

These plots show that for every case investigated, the sensitivity of actuability to absolute error in the end-effector load estimate is worse for lower payloads. This is not at all surprising: we expect a change in end-effector load of 1 kilogram to have more effect on actuability of a

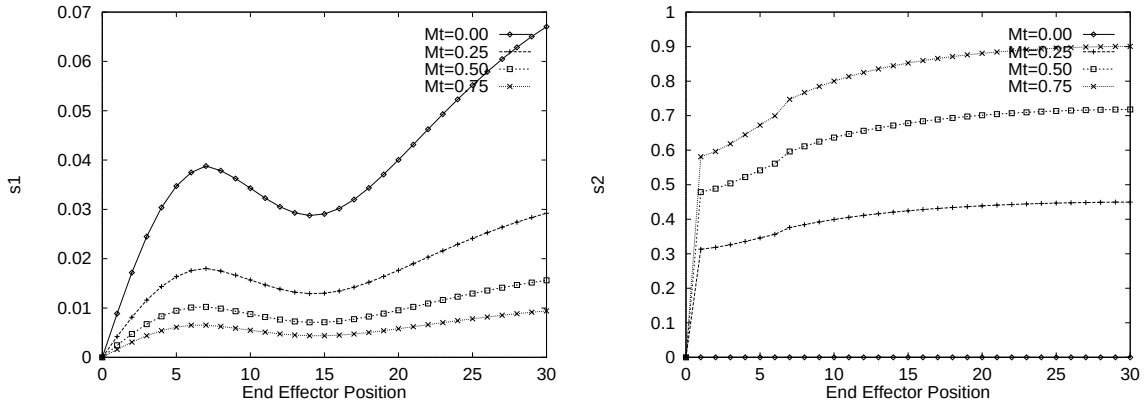


Figure 12: Sensitivities s_1 and s_2 to load mass for lower-actuated manipulator with 3 actuators

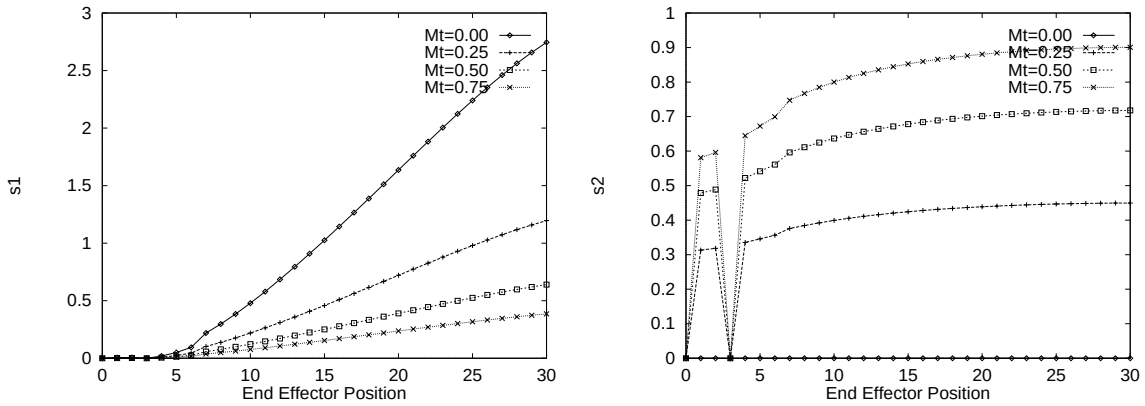


Figure 13: Sensitivities s_1 and s_2 to load mass for upper-actuated manipulator with 2 actuators

40 kilogram arm if it has a loading of zero kilograms than if it is already carrying a 10 kilogram payload. We also see from the plots that actuability is generally more sensitive to a percentage error in load magnitude when the mass of the load being carried is greater. In other words, a 10 percent change in end-effector load causes relatively more change in performance if the load is currently 40 kilograms than if the load is currently 1 kilogram. The relative sensitivities of end-effector loading were very consistent across the range of manipulators that were simulated.

4.3 Sensitivity to Kinematic Parameters

In Figures 14 and 15, we see the effects of varying the length of one link of a manipulator, without changing the location of the center of mass of the link. The plots shown are for upper- and lower-actuated four link manipulators with three actuators each.

The plots show the sensitivity of the manipulator's actuability to variations in the length of

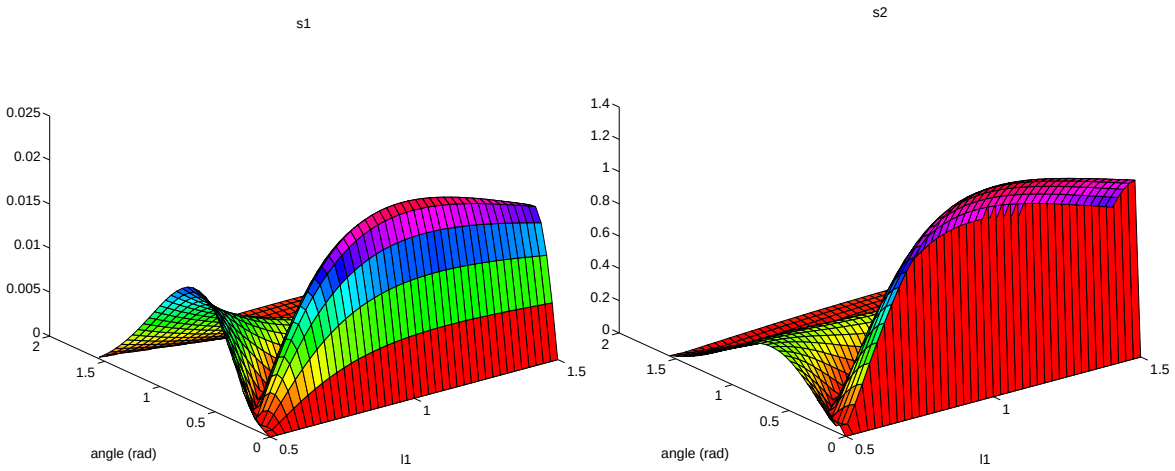


Figure 14: Sensitivities s_1 and s_2 to l_1 for lower-actuated manipulator with 3 actuators

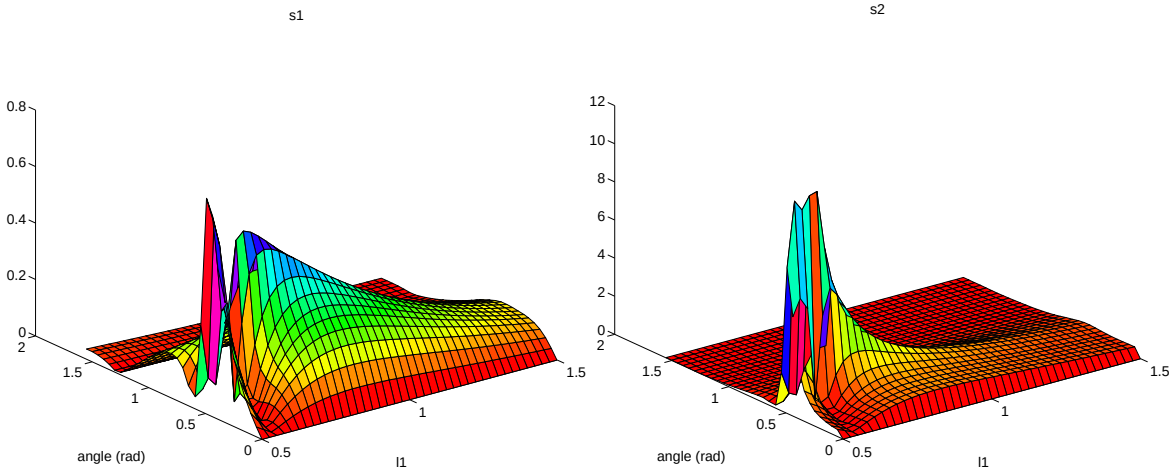


Figure 15: Sensitivities s_1 and s_2 to l_1 for lower-actuated manipulator with 3 actuators

link 1, l_1, over a range of values of l_1 and various arm positions where all the joints have the same angle. Figure 14 shows the sensitivity measures s_1 and s_2 for the lower-actuated manipulator, and Figure 15 shows the same measures for the upper-actuated manipulator. We see from Figure 14 that when l_1 is near 0.5, the lower-actuated manipulator is more sensitive to errors in l_1 while it is in curled configurations. When l_1 is between 0.75 and 1.5, the manipulator is more sensitive to errors in l_1 while it is in straighter configurations.

Figure 15 shows sensitivity data from an upper-actuated manipulator. For this manipulator, we see that that when $l_1 = 0.5$ there is an acute sensitivity to l_1 in straighter configurations. However, when l_1 is greater than 0.75, sensitivity is much lower over the entire range of configurations. This agrees with the fact that the longer we make l_1 in the lower-actuated manipulator, the more end-effector motion is due to the actuated part of the manipulator, which is generally less sensitive to modelling error than the unactuated part.

5 Conclusion

In this work, the authors have developed an index for the ability of an underactuated manipulator to generate motion at its end-effector. This index, called actuability, is a useful tool for design of underactuated manipulators, optimization of manipulator configurations, and for real-time control. The usefulness of actuability for analyzing an underactuated manipulator resembles that of the manipulability measure for conventional manipulators. We have investigated actuability analysis through actuability ellipsoids and scalar indices of actuability, and have demonstrated analysis of the sensitivity of manipulator models to parameter errors and end-effector loading. The simulation results and concepts presented here are valuable for understanding the dynamic coupling of such an underactuated system, as well as the effect of various parameters on the performance of the system.

References

[1] You-Liang Gu and Yangsheng Xu. Underactuated robot systems: Dynamic interaction and adaptive control. In *Proceedings of IEEE Systems, Man and Cybernetics Conference*, October 1994.

[2] Marcel Bergerman and Yangsheng Xu. Robust control of underactuated manipulators: Analysis and implementation. In *Proceedings of IEEE Systems, Man and Cybernetics Conference*, October 1994.

[3] S. Takashima. Control of gymnast on a high bar. In *Proceedings of IROS*, November 1991.

[4] Tsuneo Yoshikawa. *Foundations of Robotics: Analysis and Control*. The MIT Press, 1990.

[5] Hirohiko Arai, Kazuo Tanie, and Susumu Tachi. Dynamic control of a manipulator with passive joints in operational space. *IEEE Transactions on Robotics and Automation*, 9(1), February 1993.

[6] Hirohiko Arai and Susumu Tachi. Position control of a manipulator with passive joints using dynamic coupling. *IEEE Transactions on Robotics and Automation*, 7(4), August 1991.

[7] Yoshihiko Nakamura. *Advanced Robotics: Redundancy and Optimization*. Addison-Wesley Publishing Company, 1991.

[8] Mark Spong and M. Vidyasagar. *Robot Dynamics and Control*. John Wiley and Sons, 1989.

[9] Peter Lancaster. *Theory of Matricies*. Academic Press, 1969.

[10] Roger A. Horn and Charles R. Johnson. *Matrix Analysis*. Cambridge University Press, 1985.